A

Relative Quantity

plasmin (1 µg/ml) − +

B

OPG
GAPDH

plasmin (1 µg/ml) − +

C

Relative Quantity

plasmin (1 µg/ml) − + + + +
α2AP (200 nM) − − + − −
EACA (25 mM) − − − + −
Aprotinin (10 µg/ml) − − − − +

D

OPG
GAPDH

plasmin (1 µg/ml) − + + + +
α2AP (200 nM) − − + − −
EACA (25 mM) − − − + −
Aprotinin (10 µg/ml) − − − − +

E

phospho-ERK1/2
ERK1/2
phospho-p38
p38

Time (min) 0 10 30 60
plasmin (1 µg/ml) − + + +

F

OPG
GAPDH

plasmin (1 µg/ml) − + + +
PD98059 (30 µM) − − + −
SB205380 (30 µM) − − − +

G

Relative Quantity

■ Plg+/+
□ Plg−/−

H

OPG
GAPDH

Plg+/+ Plg−/−

I

Relative Quantity

□ Plg−/−

plasmin (1 µg/ml) − +

J

Plg−/−

OPG
GAPDH

plasmin (1 µg/ml) − +

tions of bone marrow tissue in the $Plg^{+/+}$ and $Plg^{-/-}$ mice was quantitatively evaluated as described under "Materials and Methods." As shown in Fig. 1F, the intensity of TRAP staining on decalcified sections of bone marrow tissue in tibias from the $Plg^{-/-}$ mice was much stronger than in those from the $Plg^{+/+}$ mice.

Effect of the Plg Deficiency on the Osteoclastogenesis of Bone Marrow-derived Cells—We evaluated how the fibronolytic system affects OC differentiation and function. The pre-OC population in bone marrow-derived cells from the $Plg^{+/+}$ and $Plg^{-/-}$ mice were evaluated after stimulation with RANKL and M-CSF, respectively. As shown in Fig. 2A, many TRAP-positive multinucleated OCs were observed in bone marrow cell cultures derived from the $Plg^{-/-}$ mice tibia. Therefore, an up-regulation of the TRAP-positive cell number in the $Plg^{-/-}$ mice-derived bone marrow cells was observed (Fig. 2B). In addition, the bone resorption activity of OCs differentiated from bone marrow-derived cells was compared in the $Plg^{+/+}$ and $Plg^{-/-}$ mice. There was an up-regulation of the bone resorption activity of $Plg^{-/-}$ mice-derived bone marrow cells (Fig. 2C). Intriguingly, plasmin significantly inhibited the M-CSF- and RANKL-induced OC differentiation of bone marrow cells derived from the $Plg^{-/-}$ and $Plg^{+/+}$ mice (Fig. 2D).

Plasmin Induced the OPG Expression in OBs—To clarify how plasmin suppresses osteoclastogenesis *in vivo*, we examined whether plasmin up-regulates the expression of OPG in OBs from the WT mice *in vitro* by qRT-PCR and a Western blot analysis. Plasmin clearly induced OPG expression in OBs from the WT mice (Fig. 3, A and B). In addition, the effect of various plasmin inhibitors (α2AP; serine protease inhibitor, aprotinin; lysine analog, ϵ-aminocaproic acid) on plasmin-induced OPG expression was investigated. These plasmin inhibitors clearly abrogated the plasmin-induced OPG expression (Fig. 3, C and D).

In addition, we examined the plasmin-stimulated phosphorylation of ERK1/2 and p38 MAPK to determine whether plasmin activates ERK1/2 and p38 MAPK in OBs. Plasmin activated ERK1/2 and p38 MAPK in OBs (Fig. 3E). We also examined whether the ERK1/2 and p38 MAPK pathways are associated with the plasmin-induced expression of OPG in OBs by using the inhibitor of MEK and p38 MAPK (PD98059 and SB203580). PD98059 and SB203580 attenuated plasmin-induced expression of OPG in OBs (Fig. 3F). These data suggest that plasmin induces OPG expression through the ERK1/2 and p38 MAPK pathways.

Moreover, qRT-PCR and a Western blot analysis revealed that the expression of OPG was suppressed in OBs from the $Plg^{-/-}$ mice (Fig. 3, G and H), thus suggesting that the absence of plasmin may result in the acceleration of osteoclastogenesis

of pre-OCs in accordance with the depletion of OPG synthesis in OBs. There was no difference in the status of RANKL mRNA expression in OBs from the $Plg^{+/+}$ and $Plg^{-/-}$ mice (data not shown). Moreover, plasmin induced OPG expression in $Plg^{-/-}$ OBs (Fig. 3, I and J).

Effects of Plg Deficiency on the Ability of OBs to Induce Osteoclastogenesis of RAW264.7 Mouse Monocyte/Macrophage Lineage Cells—The status of OC differentiation of RAW264.7 mouse monocyte/macrophage lineage cells in co-culture with $Plg^{-/-}$ OBs was examined to clarify how Plg deficiency affects OB function for osteoclastogenesis. The ability of $Plg^{-/-}$ OBs to induce OC differentiation of pre-OC RAW264.7 cells was compared with $Plg^{+/+}$ OBs. The OBs were co-cultured with RAW264.7 cells under stimulation with the inflammatory mediators interleukin 1-β (IL-1β) or prostaglandin E_2 (PGE$_2$). Inflammatory mediators induce RANKL expression on OBs (21). The inflammatory mediator-induced RANKL expression on OBs was expected to induce the osteoclastogenesis of the co-cultured RAW264.7 cells. As shown in Fig. 4A, IL-1β or PGE$_2$ increased the number of TRAP-positive multinucleated cells co-cultured with OBs. Intriguingly, the number of TRAP-positive multinucleated cells co-cultured with $Plg^{-/-}$ OBs lacking OPG expression was significantly higher than that co-cultured with $Plg^{+/+}$ OBs with or without IL-1β or PGE$_2$. In addition, the number of TRAP-positive multinucleated cells co-cultured with $Plg^{-/-}$ OBs was decreased by plasmin (Fig. 4B).

Effect of Plg Deficiency on the ALP Activity in OBs—The ALP activity in $Plg^{-/-}$ OBs was compared with $Plg^{+/+}$ OBs under stimulation with OB differentiation media as described under "Materials and Methods." The absence of Plg did not affect the ALP activity in undifferentiated and differentiated OBs (Fig. 5).

Rescue of the Down-regulated BMD in Plg-deficient Mice by the Injection of Plasmin—To clarify the effect of exogenous plasmin on bone formation *in vivo*, we evaluated the status of the BMD in the $Plg^{-/-}$ mice with or without plasmin injection. The plasmin injection clearly increased the trabecular BMD in the $Plg^{-/-}$ mice (Fig. 6A). However, the plasmin injection did not affect the cortical BMD and the weight in the $Plg^{-/-}$ mice (Fig. 6, B and C).

DISCUSSION

Fibrinolytic factors have been suggested to play an important role in bone metabolism. PAs and PAI-1 are involved in bone resorption by OCs (22, 23). However, the role of Plg/plasmin in bone metabolism was not precisely understood. This study showed that Plg/plasmin plays an important role in bone metabolism by regulating the function of both OBs and OCs.

FIGURE 3. **Plasmin induced the OPG expression in OBs.** *A–D,* OBs from the WT mice were cultured for 24 h in either the absence or presence of plasmin (1 μg/ml). Plasmin-induced expression of OPG gene in OBs from the WT mice was evaluated by qRT-PCR (A) or a Western blot analysis (B). C and D, some cultures were further treated with plasmin inhibitors as follows: α2AP (200 nM), ϵ-aminocaproic acid (25 mM), and aprotinin (10 μg/ml). The expression of OPG mRNA in OBs from the WT mice was then measured by qRT-PCR (C) or a Western blot analysis (D). E, OBs from the WT mice were stimulated with 1 μg/ml plasmin for the indicated periods. Phosphorylation of ERK1/2 and p38 MAPK was evaluated by a Western blot analysis using antibodies to ERK1/2 and p38 MAPK. F, OBs from the WT mice were pretreated with 30 μM PD98059 or 30 μM SB203580 for 60 min and then stimulated with 1 μg/ml plasmin for 24 h. The expression of OPG in OBs from the WT mice was evaluated by a Western blot analysis. G and H, OPG expression in OBs from the $Plg^{+/+}$ and $Plg^{-/-}$ mice was evaluated by qRT-PCR (G) or a Western blot analysis (H). I and J, OBs from the $Plg^{-/-}$ mice were cultured for 24 h in the absence or presence of plasmin (1 μg/ml). The OPG expression in OBs from the $Plg^{-/-}$ mice was evaluated by qRT-PCR (I) or a Western blot analysis (J). The data represent the mean of three individual experiments $\pm$ S.E. *, $p < 0.01$; **, $p < 0.05$.

936

The trabecular BMD in the tibias from the $Plg^{-/-}$ mice was significantly lower than that from the $Plg^{+/+}$ mice at 4–6 weeks after birth (Fig. 1A). In contrast, the cortical BMD in the tibias from the $Plg^{-/-}$ mice was significantly lower than that from the $Plg^{+/+}$ mice at 4–18 weeks after birth (Fig. 1B). Therefore, the decrease in the trabecular BMD in $Plg^{-/-}$ mice seemed to be transient; however, the decrease in the cortical BMD in the mice was consistently observed from the juvenile

growth period to adulthood. In addition, TRAP staining of decalcified sections of tibias from the 5-we-old mice revealed that the intensity of TRAP staining of bone marrow tissue in the tibias from the $Plg^{-/-}$ mice was significantly stronger than that from the $Plg^{+/+}$ mice (Fig. 1, E and F). Thus, the histoenzymatic assessment indicated that the OC differentiation in bone marrow tissue of the $Plg^{-/-}$ mice might be more vigorously induced than that in the $Plg^{+/+}$ mice.

The binding of RANKL to its receptor RANK triggers intricate and distinct signaling cascades that control lineage commitment and osteoclast activation (13). OPG inhibits osteoclast formation and bone resorption by blocking RANKL/RANK interactions (14). This study showed that plasmin increased the OPG expression in WT OBs (Fig. 3, A–D). Moreover, the expression level of OPG was decreased in $Plg^{-/-}$ OBs compared with $Plg^{+/+}$ OBs (Fig. 3, G and H), suggesting that absence of plasmin may result in an acceleration of OB-mediated osteoclastogenesis of pre-OCs in accordance with the depletion of OPG expression in OBs. In fact, the number of TRAP-positive multinucleated RAW264.7 cells co-cultured with $Plg^{-/-}$ OBs was significantly higher than that of the cells co-cultured with $Plg^{+/+}$ OBs (Fig. 4A). Intriguingly, plasmin significantly inhibited the M-CSF- and RANKL-induced OC differentiation of bone marrow cells derived from the $Plg^{+/+}$ and $Plg^{-/-}$ (Fig. 2D), suggesting that plasmin might attenuate osteoclastogenesis by its direct effects on pre-OCs. In addition, there was a larger population of pre-OCs in bone marrow-derived cells from the $Plg^{-/-}$ mice in comparison with the $Plg^{+/+}$ mice (Fig. 2, A–C). The level of ALP activity in $Plg^{-/-}$ OBs was similar to that in $Plg^{+/+}$ OBs (Fig. 5), thus suggesting that the bone-mineralizing activity of OBs in the $Plg^{-/-}$ mice might be comparable with that in the $Plg^{+/+}$ mice. Consequently, the $Plg^{-/-}$ mice display decreased bone mineral density in accordance with the enhanced ability of OBs to induce osteoclastogenesis of pre-OCs, the loss of the direct and suppressive effect of plasmin on pre-OCs differentiating into mature OCs, and the increased pre-OC population in bone marrow cells. In fact, the injection of plasmin into the $Plg^{-/-}$ mice clearly rescued the diminished trabecular BMD during the juvenile growth period (Fig. 6).

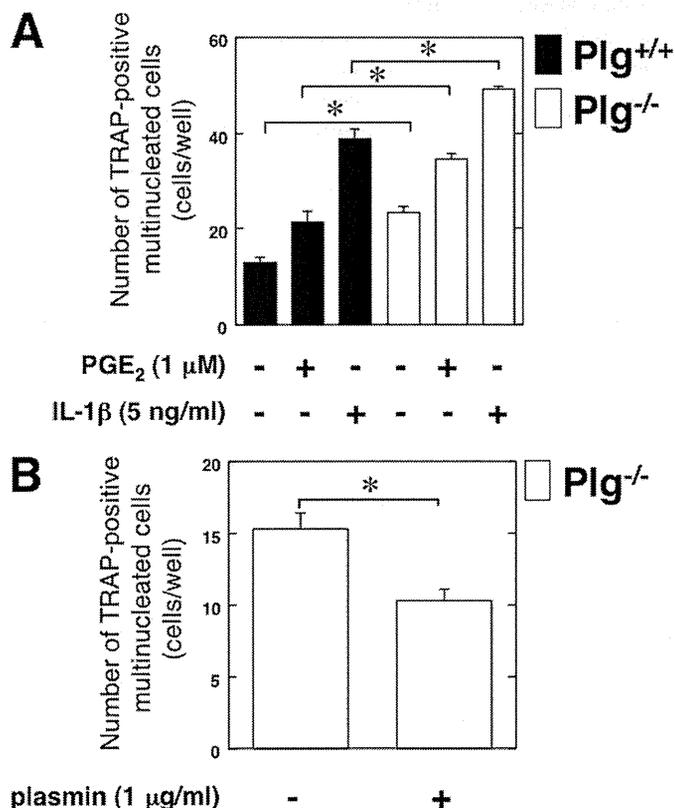FIGURE 4. **Effects of Plg deficiency on the ability of OBs to induce osteoclastogenesis of RAW264.7 cells.** *A,* RAW264.7 cells and OBs from the $Plg^{+/+}$ and $Plg^{-/-}$ mice were co-cultured for 3 days in the absence or presence of IL-1β or PGE_2. *B,* RAW264.7 cells and OBs from the $Plg^{-/-}$ mice were co-cultured for 3 days in the absence or presence of plasmin. Mature OCs were identified as multinucleated TRAP-positive cells. The number of multinucleated TRAP-positive cells was determined from six different cultures. The data represent the mean ± S.E. *, $p < 0.01$.
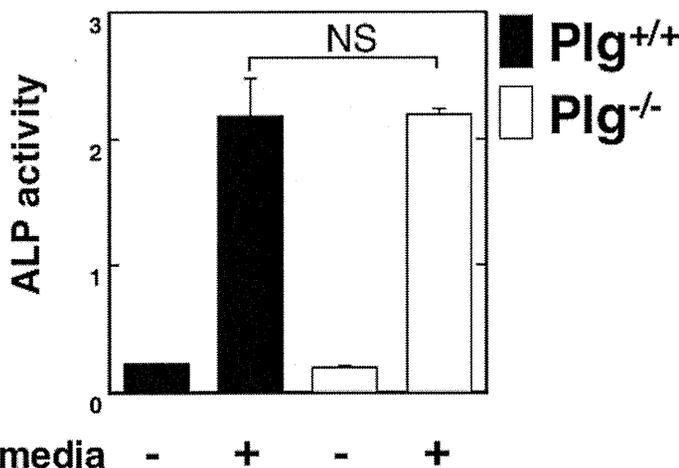

Differentiation media   -   +   -   +

FIGURE 5. **Effect of Plg deficiency on the ALP activity in OBs.** ALP activity in OBs from the $Plg^{+/+}$ and $Plg^{-/-}$ mice was evaluated ($n = 4$). The data represent the mean ± S.E. *NS,* not significant.
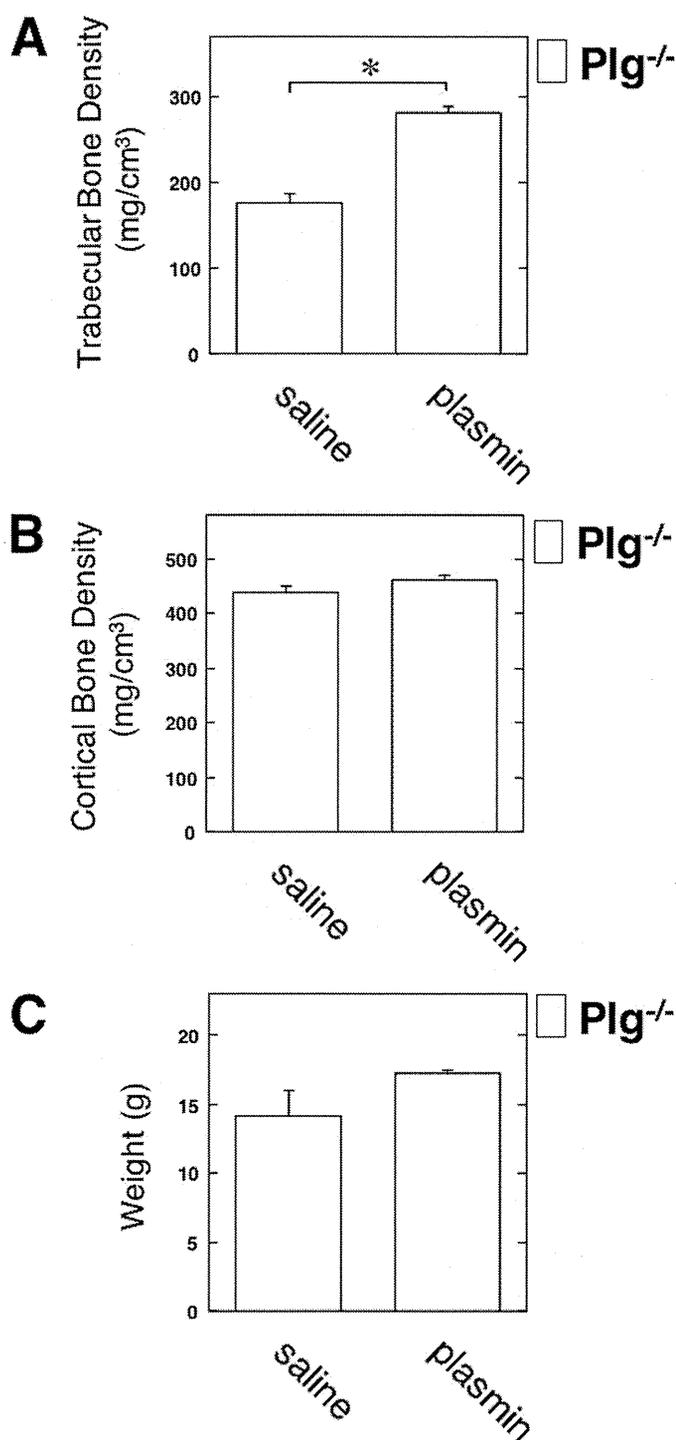
937

FIGURE 6. **Rescue of the down-regulated BMD in Plg-deficient mice by the injection of plasmin.** Intraperitoneal injection with saline or plasmin (1 mg/kg) in the 5-week-old male Plg$^{-/-}$ mice was carried out weekly for up to 3 weeks. Then the trabecular BMD (*A*), the cortical BMD (*B*), and the weight (*C*) in the male Plg$^{-/-}$ mice were measured by pQCT ($n = 3$). The data represent the mean ± S.E. *, $p < 0.01$.

causes decreased bone mineral density and decreased body weight in Plg$^{-/-}$ mice. However, plasmin directly activates various intracellular signaling through annexin A2 in macrophage (26). Plasmin activates macrophages via the annexin A2 heterotetramer composed of annexin A2 and S100A10 with subsequent stimulation of Janus kinase JAK1/TYK2 signaling. JAK1/TYK2 leads to STAT3 activation, Akt-dependent nuclear factor-κB (NF-κB) activation, and phosphorylation of ERK1/2 and p38 MAPK. Furthermore, inhibitors of JAK, p38 MAPK, and NF-κB revealed that these signaling pathways are indispensable for the plasmin-mediated tumor necrosis factor-α and IL-6 induction in the cells. In addition, angiostatin, a fragment of plasmin(ogen), is a ligand and an antagonist for integrin α9β1 (27). Angiostatin, representing the kringle domains of plasmin, alone did not induce the migration of Chinese hamster ovary (CHO) cells, but simultaneous activation of the G protein-coupled protease-activated receptor-1 with an agonist peptide induced the migration on angiostatin. These facts suggest that plasmin directly stimulates various cell lineages without an indirect cell stimulation through an activation of some growth factors such as TGF-β. We showed that plasmin activated ERK1/2 and p38 MAPK, and the inhibition of ERK1/2 and p38 MAPK attenuated plasmin-induced OPG expression (Fig. 3, *E* and *F*). In addition, plasmin activated JNK, but the inhibition of JNK did not attenuate plasmin-induced OPG expression (data not shown). These data suggest that plasmin induces OPG expression through the ERK1/2 and p38 MAPK pathways. However, the time lag between the activation of p38 MAPK and ERK1/2 after plasmin stimulation in OBs might depend on the hierarchy of ERK1/2 and p38 MAPK in the plasmin-induced signal transduction. The ERK1/2 might be the downstream target of p38 MAPK directly activated by plasmin in OBs. Further investigations would be required to clarify the details.

These results strongly suggest that the plasmin activity regulates both OB and OC functions and then plays an important role in bone metabolism. These findings may provide new insights into the development of clinical therapies for the prevention of bone loss-related disorders.

REFERENCES

1. Braaten, J. V., Handt, S., Jerome, W. G., Kirkpatrick, J., Lewis, J. C., and Hantgan, R. R. (1993) *Blood* **81,** 1290–1299
2. Lijnen, H. R., De Cock, F., Van Hoef, B., Schlott, B., and Collen, D. (1994) *Eur. J. Biochem.* **224,** 143–149
3. Carmeliet, P., and Collen, D. (1996) *Semin. Thromb. Hemost.* **22,** 525–542
4. Matsuno, H., Ishisaki, A., Nakajima, K., Okada, K., Ueshima, S., Matsuo, O., and Kozawa, O. (2003) *Blood* **102,** 3621–3628
5. Kanno, Y., Kuroki, A., Minamida, M., Kaneiwa, A., Okada, K., Tomogane, K., Takeuchi, K., Ueshima, S., Matsuo, O., and Matsuno, H. (2008) *Thromb. Res.* **123,** 336–341
6. Kanno, Y., Hirade, K., Ishisaki, A., Nakajima, K., Suga, H., Into, T., Matsushita, K., Okada, K., Matsuo, O., and Matsuno, H. (2006) *J. Thromb. Haemost.* **4,** 1602–1610
7. Kanno, Y., Kuroki, A., Okada, K., Tomogane, K., Ueshima, S., Matsuo, O., and Matsuno, H. (2007) *J. Thromb. Haemost.* **5,** 2266–2273
8. Kanno, Y., Kaneiwa, A., Minamida, M., Kanno, M., Tomogane, K., Takeuchi, K., Okada, K., Ueshima, S., Matsuo, O., and Matsuno, H. (2008) *J. Invest. Dermatol.* **128,** 2792–2797
9. Kanno, Y., Kawashita, E., Minamida, M., Kaneiwa, A., Okada, K., Ueshima, S., Matsuo, O., and Matsuno, H. (2010) *Am. J. Pathol.* **176,** 238–245
10. Daci, E., Everts, V., Torrekens, S., Van Herck, E., Tigchelaar-Gutterr, W.,

Plasmin activates a latent transforming growth factor β (TGF-β) (24, 25) trapped in extracellular matrix to induce an OPG expression in extracellular matrix-harbored OBs. The accelerated expression of OPG on OBs might result in the suppression of the OB-mediated osteoclastogenesis. It is under investigation by us whether deficiency of activated TGF-β

938

Bouillon, R., and Carmeliet, G. (2003) *J. Bone Miner. Res.* **18**, 1167–1176

11. Daci, E., Verstuyf, A., Moermans, K., Bouillon, R., and Carmeliet, G. (2000) *J. Bone Miner. Res.* **15**, 1510–1516

12. Furlan, F., Galbiati, C., Jorgensen, N. R., Jensen, J. E., Mrak, E., Rubinacci, A., Talotta, F., Verde, P., and Blasi, F. (2007) *J. Bone Miner. Res.* **22**, 1387–1396

13. Wada, T., Nakashima, T., Hiroshi, N., and Penninger, J. M. (2006) *Trends Mol. Med.* **12**, 17–25

14. Hofbauer, L. C., and Heufelder, A. E. (2001) *J. Mol. Med.* **79**, 243–253

15. Li, J., Sarosi, I., Yan, X. Q., Morony, S., Capparelli, C., Tan, H. L., McCabe, S., Elliott, R., Scully, S., Van, G., Kaufman, S., Juan, S. C., Sun, Y., Tarpley, J., Martin, L., Christensen, K., McCabe, J., Kostenuik, P., Hsu, H., Fletcher, F., Dunstan, C. R., Lacey, D. L., and Boyle, W. J. (2000) *Proc. Natl. Acad. Sci. U.S.A.* **97**, 1566–1571

16. Ploplis, V. A., Carmeliet, P., Vazirzadeh, S., Van Vlaenderen, I., Moons, L., Plow, E. F., and Collen, D. (1995) *Circulation* **92**, 2585–2593

17. Suda, T., Jimi, E., Nakamura, I., and Takahashi, N. (1997) *Methods Enzymol.* **282**, 223–235

18. Kanazawa, S., Ota, S., Sekine, C., Tada, T., Otsuka, T., Okamoto, T., Sønderstrup, G., and Peterlin, B. M. (2006) *Proc. Natl. Acad. Sci. U.S.A.* **103**, 14465–14470

19. Nishiwaki, T., Yamaguchi, T., Zhao, C., Amano, H., Hankenson, K. D., Bornstein, P., Toyama, Y., and Matsuo, K. (2006) *J. Bone Miner. Res.* **21**, 596–604

20. Kanno, Y., Into, T., Lowenstein, C. J., and Matsushita, K. (2008) *Cardiovasc. Res.* **77**, 221–230

21. Nakashima, T., Kobayashi, Y., Yamasaki, S., Kawakami, A., Eguchi, K., Sasaki, H., and Sakai, H. (2000) *Biochem. Biophys. Res. Commun.* **275**, 768–775

22. Daci, E., Udagawa, N., Martin, T. J., Bouillon, R., and Carmeliet, G. (1999) *J. Bone Miner. Res.* **14**, 946–952

23. Everts, V., Daci, E., Tigchelaar-Gutter, W., Hoeben, K. A., Torrekens, S., Carmeliet, G., and Beertsen, W. (2008) *Bone* **43**, 915–920

24. Thirunavukkarasu, K., Miles, R. R., Halladay, D. L., Yang, X., Galvin, R. J., Chandrasekhar, S., Martin, T. J., and Onyia, J. E. (2001) *J. Biol. Chem.* **276**, 36241–36250

25. Lyons, R. M., Gentry, L. E., Purchio, A. F., and Moses, H. L. (1990) *J. Cell Biol.* **110**, 1361–1367

26. Li, Q., Laumonnier, Y., Syrovets, T., and Simmet, T. (2007) *Arterioscler. Thromb. Vasc. Biol.* **27**, 1383–1389

27. Majumdar, M., Tarui, T., Shi, B., Akakura, N., Ruf, W., and Takada, Y. (2004) *J. Biol. Chem.* **279**, 37528–37534

939

1   Title: E-selectin Mediates *Porphyromonas gingivalis* Adherence to Human Endothelial

2   Cells.

3

4   Running Title: *P. GINGIVALIS* INTERACTS WITH E-SELECTIN.

5

6   Authors: Toshinori Komatsu,[1,2] Keiji Nagano,[3] Shinsuke Sugiura,[1] Makoto Hagiwara,[1]

7   Naomi Tanigawa,[1] Yuki Abiko,[3] Fuminobu Yoshimura,[3] Yasushi Furuichi,[2] and Kenji

8   Matsushita[1,2]*

9

10   Departments of Oral Disease Research, National Center for Geriatrics and Gerontology at

11   Obu, Aichi 474-8511, Japan,[1] Department of Periodontology and Endodontology, School of

12   Dentistry, Health Sciences University of Hokkaido, Ishikari, Hokkaido 061-0293, Japan,[2]

13   Department of Microbiology, School of Dentistry, Aichi-Gakuin University, Nagoya, Aichi

14   464-8651, Japan[3]

15

16   *Corresponding author. Mailing address: Department of Oral Disease Research, National

17   Institute for Longevity Science, National Center of Geriatrics and Gerontology, Obu, Aichi

18   747-8511, Japan. Phone: +81-562-46-2311. Fax: +81-562-46-8479. E-mail:

19   kmatsu30@ncgg.go.jp

20

21

22 **ABSTRACT**

23 *Porphyromonas gingivalis*, a major periodontal pathogen, may contribute to atherogenesis

24 and other inflammatory cardiovascular diseases. However, little is known about interactions

25 between *P. gingivalis* and endothelial cells. E-selectin is a membrane protein on endothelial

26 cells that initiates recruitment of leukocytes to inflamed tissue, and it may also play a role in

27 pathogen attachment. In the present study, we examined the role of E-selectin in *P.*

28 *gingivalis* adherence to endothelial cells. Human umbilical vein endothelial cells

29 (HUVECs) were stimulated with TNF-α to induce E-selectin expression. Adherence of *P.*

30 *gingivalis* to HUVECs was measured by fluorescent microscopy. TNF-α increased

31 adherence of wild-type *P. gingivalis* to HUVECs. An antibody to E-selectin and sialyl

32 Lewis X suppressed *P. gingivalis* adherence to stimulated HUVECs. *P. gingivalis* mutants

33 lacking OmpA-like proteins Pgm6/7 had reduced adherence to stimulated HUVECs, but

34 fimbriae-deficient mutants were not affected. E-selecin-mediated *P. gingivalis* adherence

35 activated endothelial exocytosis. These results suggest that the interaction between host

36 E-selectin and pathogen Pgm6/7 mediates *P. gingivalis* adherence to endothelial cells and

37 may trigger vascular inflammation.

38

39 **Key Words:** periodontitis, atherogenesis, outer membrane protein, vascular inflammation

40

41 **INTRODUCTION**

42   Periodontitis is a disease of the supporting structures of the teeth, causing loss of

43 attachment to the alveolar bone and eventual exfoliation of teeth (5) . Severe periodontitis

44 affects up to 20% of the population, and mild-to-moderate periodontitis is observed in the

45 majority of adults (6) . Gram-negative bacteria play an important role in the pathogenesis of

46 human periodontal diseases (15) (42) and *Porphyromonas gingivalis* is one of the species

47 most strongly implicated in periodontal diseases (14) (43) . Several recent studies have

48 demonstrated that *P. gingivalis* is able to invade and activate different cell types in the tissue

49 surrounding teeth (endothelial and gingival epithelial cells as well as periodontal ligament

50 cells) (12) (26) (40) . Moreover, recent studies have demonstrated a transient bacteremia

51 with potential systemic infection after a variety of dental treatment procedures (2) (19) (20)

52 (41) . Endothelial cells, therefore, can act as primary target cells during infection with *P.*

53 *gingivalis*. However, little is known about mechanisms of infection and activation of

54 endothelial cells by *P. gingivalis*.

55   The endothelium has several important functions that include providing a

56 nonadhesive, nonthrombotic barrier between the blood and the underlying tissues. In

57 atherosclerosis, or in response to injury or inflammatory cytokines such as tumor necrosis

58 factor α (TNF-α), the endothelium becomes activated and selectins and cell adhesion

59 molecules (CAMs) are rapidly induced (39) (36). In particular, members of the

60 immunoglobulin superfamily of CAMs, such as intercellular cell adhesion molecule-1

61 (ICAM-1) and vascular cell adhesion molecule-1 (VCAM-1), as well as selectin family

62 members, E-selectin and P-selectin, are expressed and play crucial roles in the adhesion and

63 migration of monocyte/macrophage infiltration into atherosclerotic lesions during the early

64 and subsequent stages of atherosclerosis in a variety of animal models (47) (21) (49).

65 Increased expression of E-selectin and production of pro-inflammatory cytokines in the

66   endothelium play a pivotal role in the generation of leukocyte infiltrates and subsequent

67   atherosclerotic plaque formation (28) (16). *P. gingivalis* infection significantly increases

68   endothelial expression of VCAM-1, ICAM-1 and E-selectin, enhances production of IL-6,

69   IL-8 and MCP-1, and increases adhesion of THP-1 monocytes to endothelial cells (46) (18) .

70   Therefore, *P. gingivalis* elicits a pro-atherogenic response in endothelial cells.   Although

71   E-selectin is involved in vascular inflammation and is induced with *P. gingivalis*, interaction

72   between *P. gingivalis* and endothelial cells is not understood.   In the present study, we

73   explored the ability of E-selectin to facilitate *P. gingivalis* adherence to human umbilical vein

74   endothelial cells (HUVECs).   We found that activated endothelial cells interact with *P.*

75   *gingivalis* via E-selectin on endothelial cells and via OmpA-like proteins Pgm6/7 of the

76   bacteria.

77

78 **MATERIALS AND METHODS**

79   **Bacterial strains and growth conditions.** *P. gingivalis* ATCC 33277 was used

80 as a wild-type strain in this study. *P. gingivalis* defective mutants lacking *fimA* were

81 constructed as described previously (17). A *P. gingivalis* Pgm6/7-deficient mutant was

82 constructed as described previously (32). This mutant did not show any sign of a

83 polar effect on the downstream gene (data not shown). All *P. gingivalis* strains

84 were grown at 37 °C under anaerobic conditions (10% CO_2, 10% H_2, and 80% N_2) on

85 *Brucella* HK agar (Kyokuto Pharmaceutical Industrial Co., Ltd., Tokyo, Japan)

86 supplemented with 5% laked rabbit blood, haemin (2.5 µg/ml), menadione (5 µg/ml) and

87 dithiothreitol (0.1 mg/ml) and in trypticase soy broth (BD, Franklin Lakes, NJ)

88 supplemented with yeast extract (2.5 mg/ml), haemin (2.5 µg /ml), menadione (5 µg/ml)

89 and dithiothreitol (0.1 mg/ml). Bacterial growth was monitored by measuring OD_{660}.

90 For infection assays, an infection ratio (multiplicity of infection) of 100 bacteria per cell

91 was added to the cell culture medium.

92   **Cell culture conditions.** Human umbilical vein endothelial cells (HUVECs)

93 were cultured in endothelial cell growth medium-2 (EGM-2) (Lonza, Basel, Switzerland)

94 supplemented with fetal bovine serum, hydrocortisone, human recombinant fibroblast

95 growth factor, vascular endothelial growth factor, recombinant insulin growth factor-1,

96 ascorbic acid, human recombinant epidermal growth factor, gentamicin, and amphotericin B

97 at 37°C in an atmosphere of 5% CO_2. Cells were cultured in 75-cm^2 flasks at 37°C in a

98 humidified atmosphere of 5% CO_2. Both HCAECs and CASMCs were cryopreserved at the

99 third passage and were passaged an additional two or three times before use.

100   **E-selectin expression.** E-selectin cDNA was constructed as described

101 previously (53). The E-selctin cDNA was amplified by PCR with specific primers (5'-gac

102 agc tag cat gat tgc ttc aca g-3', including an additional Nhe site, and 5'-cgg cct cga gtt aaa gga

103   tgt aag aag gc-3', including an additional Xho site) and cloned into pcDNA3.1 vector

104   (Invitrogen, Carlsbad, CA).   For preparation of a soluble E-selectin vector, a stop codon and

105   unique EcoRV site were introduced by site-directed mutagenesis (Promega, Madison, WI)

106   into the boundary between the sixth consensus repeat and the transmembrane domain using

107   the following oligonucleotide, which starts at nucleotide 1776: 5"CC AAC   ATT   CCC

108   TAG   ATA   TCT   AGA   CTT   TCT   GCT   G-3'.

109   **Measurement of E-selectin production.**   An ELISA-based method was used for

110   quantification of E-selectin protein expression in endothelial cells.   HUVECs (3.5×10^5

111   cells/ml) were seeded into 6-well plates and grown overnight.   Then the cells were

112   stimulated with 10 ng/ml of TNF-α (PeproTec Inc., Rocky Hill, NJ) for 1, 2, 3, 4, 8, and 24

113   h.   After removing the media, the cell layers were washed twice with PBS.   Cells were

114   lysed in a cell lysis reagent (CelLytic P, Sigma-Aldrich, St. Louis, MO) with protease

115   inhibitor mixture (Nacalai Tesque, Kyoto, Japan).   Concentrations of E-selectin in the cell

116   lysates were determined using a commercial ELISA kit for E-selectin (eBioscience, San

117   Diego, CA).   The cell lysates were also mixed with 4x Laemmli sample buffer without

118   reducing agents and were fractionated on a 7.5% SDS-PAGE and immunoblotted with a

119   monoclonal antibody to E-selectin (BBIG-E4 (5D11): R&D Systems, Abingdon, U.K.).

120   **Analysis of *P. gingivalis* adhesion to endothelial cells.**   HUVECs (2×10^6 cells)

121   were seeded in a Lab-Tek II Chamber Slide System (Nalge Nunc International, Rochester,

122   NY) that has been coated with 50 mg/ml of rat tail collagen (BD) and the cells were

123   incubated for 24 h before administration of *P. gingivalis*.   HUVECs grown to near

124   confluence per well were stimulated with TNF-α for 3 h and then *P. gingivalis* cells, which

125   had been washed with EGM-2 and resuspended in EGM-2 without an antibiotic at a

126   concentration of 10^8 cells/ml, were added to the monolayer cells at an MOI of 1:100 under

127   5% CO2 at 37°C for 0.5-3 h.   Cells were then washed three times with PBS, followed

128   each time by gentle rinsing for 5 min at room temperature, and fixed with 4% (w/v)

129   paraformaldehyde at 4℃ overnight. After washing three times with PBS, the cells were

130   permeabilized with PBS containing 0.05% Triton-X-100 at room temperature for 30 min.

131   They were washed again and then blocked with PBS containing 5% (w/v) BSA at room

132   temperature for 30 min.   Bacterial cells on chamber slides were labeled with an antiserum

133   for *P. gingivalis* whole-cells (1: 1000 dilution) for 60 min at room temperature and washed

134   five times with PBS.   Then the bacterial cells were incubated with Alexa Fluor 488 goat

135   anti-rabbit IgG (1:1000 dilution, Invitrogen Co., Carlsbad, CA).   Actin filaments in

136   HUVECs or 293 cells were simultaneously stained with Alexa Fluor 568 phalloidin (1

137   μg/ml, Invitorgen Co.) for 60 min at room temperature in the dark.   After washing 10

138   times with PBS, chamber slides were mounted onto a slide containing ProLong Gold

139   antifade reagent (Invitrogen).   Adherent bacteria on the cell surface were examined by

140   fluorescent microscopy (Keyence, Osaka, Japan).   We measured the area stained with

141   Alexa488 (corresponding to *P. gingivalis*) in a visual field (corresponding to 0.06 mm^2) by

142   using Image J program.   We then calculated bacterial number by dividing the area by the

143   size (pixel) of a *P. gingivalis* cell.   To determine whether E-selectin is involved in *P.*

144   *gingivalis* adherence to endothelial cells, TNF-α-pretreated HUVECs were incubated with *P.*

145   *gingivalis* ATCC 33277 (10^8 cells/ml/well) for 30 min-3 h in the presence of various

146   concentrations of an antibody for E-selectin (R&D Systems, Inc., Minneapolis, MN),

147   recombinant E-selectin, and Sialyl Lewis X (Calbiochem, San Diego, CA).   *P. gingivalis*

148   ATCC 33277 (10^8 cells/ml/well) was also incubated with HEK 293 cells transfected with a

149   human E-selectin-inserted vector for 30 min.   To explore ligands for E-selctin on *P.*

150   *gingivalis*, *P. gingivalis* ATCC 33277 (wild type), FimA-deficient mutant (Δ*fimA*), and

151   Pgm6/7-deficient mutant (Δ*pgm6/7*) (10^8 cells/ml) were incubated with TNF-α-pretreated

152   HUVECs for 3 h, respectively.   TNF-α-pretreated HUVECs were incubated with *P.*

153   *gingivalis* ATCC 33277 (10^8 cells/ml) for 30 min in the presence or absence of envelopes

154   isolated from wild-type or mutant *P. gingivalis*. TNF-α-pretreated HUVECs were

155   incubated with *P. gingivalis* ATCC 33277 (10^8 cells/ml) for 30 min in the presence or

156   absence of purified FimA fimbriae and Pgm6/7.

157   **Measurement of VWF and nitric oxide.**   HUVECs (3.5×10^5 cells/ml) were

158   seeded into 12-well plates and grown overnight.   Then the cells were stimulated with 10

159   ng/ml of TNF-α for 3 h.   *P. gingivalis* cells were inoculated into cultures at an MOI of 100

160   and the cultures were incubated for 30 min and 1 h.   The culture media were then

161   collected and centrifuged at 13,000 rpm for removing bacterial cells.   Concentrations of

162   VWF in the supernatants were measured using ELISA according to the manufacturer's

163   instructions (VWF ELISA kit, American Diagnostic Inc, Stanford, CT).   The

164   concentration of NO_2^-/NO_3^- was also measured by 2,3-diaminonapthalene (DAN) assay

165   (24).

166   **Preparation of *P. gingivalis* envelope.**   Separation of whole envelopes and the

167   outer membrane from *P. gingivalis* strains was performed essentially as described previously

168   (30).   Briefly, bacterial cells were washed with PBS (pH 7.5) containing 0.15 M NaCl and

169   then resuspended with PBS (pH 7.5) containing 0.1 mM *N*-α-*p*-tosyl-L-lysine chloromethyl

170   ketone, 0.2 mM phenylmethylsulfonyl fluoride, and 0.1 mM leupeptin. The cells were

171   disrupted by sonication, and the remaining undisrupted bacterial cells were removed by

172   centrifugation at 1,000 x *g* for 10 min. The envelope was collected as a pellet by

173   centrifugation at 100,000 x *g* for 60 min at 4°C. The pellet was washed once by resuspension

174   in PBS and recentrifuged.   The final pellet was suspended in PBS.

175   **Purification of FimA.**   Major fimbriae from *P. gingivalis* ATCC 33277 was

176   purified as described previously (52).   The purity was ascertained by scanning of the

177   stained sodium dodecyl sulfate (SDS)-polyacrylamide gel.

178   **Purification of Pgm6/7 complex.**   Functional Pgm6/7 complex was purified by

179   two methods.   First, we purified it electrophoretically from bacterial envelopes as

180   previously reported (32).   Briefly, an envelope fraction of *P. gingivalis* was subjected to

181   SDS-PAGE under non-reducing conditions.   A 120-kDa protein band, corresponding to

182   Pgm6/7 heterotrimer, was excised, and then the complex was extracted electrically from a

183   piece of gel.   We used these samples for experiments of Figure 3E and supplemental

184   data#3B.   Second, we constructed C-terminally hexahistidine-tagged Pgm6 and purified

185   Pgm6/7 complex by using a nickel affinity column from a *P. gingivalis* mutant.   Briefly, we

186   inserted a DNA fragment consisting of *pgm6 orf* associated with the DNA sequence encoding

187   Gly-Ser-Ser-hexahistidine into the vector pT-COW (13) bearing a powerful promoter of the

188   350-bp upper region of *ragA* (31).   The constructed plasmid was introduced into a

189   *pgm6*-deletion mutant of *P. gingivalis* (32).   The cell lysate was applied to a nickel affinity

190   column and the bound proteins were eluted.   Although a hexahistidine tag was associated

191   with Pgm6 alone, Pgm6/7 complex was obtained.   We used these samples for experiments

192   of Figure 3F, 3G, and supplemental data #3C.

193

194

195 **RESULTS**

196 **TNF-α augments adherence of *P. gingivalis* to endothelial cells through**

197 **inducing expression of E-selectin.** We first examined induction of E-selectin expression

198 by TNF-α using ELISA and Western blotting in HUVEC cultures. TNF-α induced a

199 time-dependent expression of E-selectin in HUVECs (supplemental data #1, #2). E-selectin

200 expression was maximal at 3 h after TNF-α addition. No basal expression of E-selectin was

201 found. To determine whether E-selectin expression in endothelial cells is involved in

202 adhesion of *P. gingivalis* to the cells, we incubated HUVECs with TNF-α (10 ng/ml) for 0.5-3

203 h, and then *P. gingivalis* ATCC 33277 cells (10^8 cells/ml/well) were added to the culture

204 medium for 0.5-3 h. Cells were then washed and attachment of *P. gingivalis* to the cells was

205 observed by fluorescent microscopy. Attachment of *P. gingivalis* to HUVECs increased

206 time-dependently without pretreatment of TNF-α (Figures 1A, B). Pretreatment with 10

207 ng/ml of TNF-α significantly enhanced the level of attachment in HUVEC cultures.

208 To clarify the role of E-selectin in *P. gingivalis* adherence to HUVECs, we examined the

209 effect of anti-E-selectin antibodies on *P. gingivalis* adherence to HUVECs. HUVECs were

210 pretreated with TNF-α and were then incubated with *P. gingivalis* for 30 min in the presence

211 of antibodies for E-selectin or control IgG. An antibody to E-selectin inhibited *P. gingivalis*

212 adherence to TNF-α-pretreated HUVECs (Figure 2A).

213 E-selectin mediates the rolling of leukocytes on activated endothelial cells through

214 binding of the carbohydrate antigen sialyl Lewis X (37). Therefore, we examined the effect

215 of sialyl Lewis X on interactions between *P. gingivalis* and endothelial cells. Sialyl Lewis

216 X inhibited TNF-α-induced *P. gingivalis* adherence to HUVECs at a concentration of 0.1

217 μg/ml (Figure 2B). To assess the effect of E-selectin over-expression on the up-regulation

218 of *P. gingivalis* adherence to endothelial cells, we transfected a E-selectin-inserted plasmid

219 into HUVECs. Expression of E-selectin was confirmed by Western blotting 24 h after

220   transfection (Figure 2C).   Adherence of *P. gingivalis* significantly increased in

221   E-selectin-transfected HEK 293 cells (Figure 2D).   These results suggest that

222   TNF-α augments *P. gingivalis* adherence to HUVECs through inducing expression of

223   E-selectin.

224   **P. gingivalis interacts with TNF-α-stimulated endothelial cells via its ~~outer-~~**

225   **~~membrane protein~~ Pgm6/7.**   The initial adherence of *P. gingivalis* to host cells is mediated

226   by multiple adhesins including FimA and HagB (44) (45).   To determine whether an

227   interaction between major fimbriae occurs with E-selectin, we examined adherence to

228   endothelial cells of *P. gingivalis* defective in FimA alone (ΔFimA).   TNF-α increased the

229   adherence to endothelial cells of FimA-deficient *P. gingivalis* as well as wild-type *P.*

230   *gingivalis* and the degrees of adherence were similar (Figures 3A, B).   We next examined

231   whether a major outer membrane protein of *P. gingivalis* that which is homologous to OmpA

232   protein in *Escherichia coli*, Pgm6/7, mediates *P. gingivalis* mediates adherence to HUVECs.

233   The Pgm6/7-deficient mutant (ΔPgm6/7) was incubated with TNF-α-pretreated HUVECs

234   and attachment of *P. gingivalis* to the cells was observed. TNF-α increased adherence of

235   wild-type *P. gingivalis* to endothelial cells but failed to increase adherence of ΔPgm6/7 *P.*

236   *gingivalis* to endothelial cells (Figure 3C).   To clarify whether Pgm6/7 mediates *P.*

237   *gingivalis* adherence to HUVECs, we prepared envelopes from wild-type, ΔFimA, and

238   ΔPgm6/7 *P. gingivalis* and examined the effects on interaction between wild-type *P.*

239   *gingivalis* and HUVECs.   Envelope peptides from wild-type *P. gingivalis* or ΔFimA *P.*

240   *gingivalis* suppressed adherence of *P. gingivalis* to TNF-α-pretreated HUVECs (Figure 3D).

241   However, envelope peptides from ΔPgm6/7 *P. gingivalis* did not affect *P. gingivalis*

242   adherence.   In addition, the Pgm6/7 fraction from *P. gingivalis* ATCC 33277 suppressed

243   TNF-α-augmented *P. gingivalis* adherence, but the FimA fraction from the same strain did

244   not (Figure 3E).   Furthermore, purified Pgm6/7 inhibited TNF-α activation of *P. gingivalis*

245   adherence to HUVECs at a concentration as low as 0.25 ng/ml (Figure 3F, G).   These results

246   suggest that the *P. gingivalis* peptide Pgm6/7 plays a role in the adherence of *P. gingivalis* to

247   endothelial cells.

248   **P. gingivalis interaction with endothelial cells via E-selectin induces**

249   **endothelial exocytosis and NO production.**   Finally, to determine whether

250   E-selectin-mediated adherence of *P. gingivalis* activates endothelial cells and increses

251   vascular inflammation, we investigated induction of vWF and nitric oxide in TNF-α-

252   pretreated endothelial cells by stimulation with *P. gingivalis*.   HUVECs were incubated with

253   TNF-α (10 ng/ml) for 3 h and then the cells were washed and incubated with *P. gingivalis* for

254   0-1 h.   Then release of vWF into the media was measured by ELISA.   *P. gingivalis* triggers

255   endothelial exocytosis, as measured by endothelial release of VWF.   Release of vWF by

256   stimulation with *P. gingivalis* was also enhanced by pretreatment of HUVECs with TNF-α

257   (Figure 4).   TNF-α pretreatment of HUVECs before *P. gingivalis* stimulation for 30 min

258   significantly increased NO_2^- release into the media (Figure 5).   An anti-E-selectin antibody

259   also-inhibited activation by *P. gingivalis* of NO release from TNF-α-pretreated HUVECs.

260   These results suggest that *P. gingivlis* interaction with endothelial cells via E-selectin

261   activates the endothelial cells and enhances proinflammatory responses of the cells to the

262   bacteria.

263 **DISCUSSION**

264　　　*P. gingivalis* adherence to and invasion of endothelial cells has been reported by

265 several investigators (46) (9) . However, this is the first report on the adhesion of activated

266 endothelial cells by *P. gingivalis*. HUVECs activated with TNF-α increased the adherence

267 of *P. gingivalis* through E-selectin expression, interacting with the OmpA-like proteins

268 Pgm6/7 in *P. gingivalis*.

269　　　One of the initial events in atherogenesis is the activation of endothelial cells,

270 which then express cell surface adhesion molecules such as endothelial leukocyte adhesion

271 molecule (E-selectin), vascular cell adhesion molecule (VCAM-1), and intercellular

272 adhesion molecule (ICAM-1) (10) (22) (8). These endothelial adhesion molecules in turn

273 facilitate the attachment of blood leukocytes to endothelial surfaces (34). In the present study,

274 we demonstrated that one of the periodontopathogens adhere to endothelial cells via

275 E-selectin.

276　　　*P. gingivalis* can invade many cell types, including human oral epithelial cells (33)

277 (51), human gingival fibroblasts or epithelial cells (3) (26), human coronary artery smooth

278 muscle cells, and human coronary artery endothelial (HCAE) cells (11). Adhesion of *P.*

279 *gingivalis* to host cells is multimodal (27) and involves a variety of cell surface and

280 extracellular components, including fimbriae, proteases, hemagglutinins, and

281 lipopolysaccharides (LPS) (8). Among the large array of virulence factors produced by *P.*

282 *gingivalis*, the major fimbria (FimA), as well as cysteine proteinases (gingipains), contribute

283 to the attachment to and invasion of many types of mammalian cells including oral epithelial

284 cells (4) and endothelial cells. *P. gingivalis* strains deficient in FimA fimbriae had

285 attenuated capacity to adhere to and invade epithelial cells and endothelial cells (33) (46)

286 (51) . Invasive *P. gingivalis* strains and their purified fimbriae activates expression of

287 cytokines and cell adhesion molecules in endothelial cells (46) . However, our data showed

288   that Pgm6/7 rather than FimA is associated with *P. gingivalis* adherence to TNF-α-treated

289   endothelial cells. Although we do not know exact mechanisms, *P. gingivalis* cells adhere to

290   activated endothelial cells through their Pgm6/7 in a manner different from the

291   fimbriae-integrin interaction. TNF-α activates endothelial cells to express adhesion

292   molecules as well as proinflammatory cytokine and chemokine receptors and promotes

293   synthesis and release of a variety of inflammatory cytokines and chemokines to thereby

294   support recruitment of activated leukocytes to an inflammatory lesion (38). TNF-α promotes

295   the inflammatory cascade within the arterial wall during development of atherosclerosis (1).

296   In addition, *P. gingivalis* has been detected within atherosclerotic plaques from vascular

297   tissues (54) (25). Therefore, TNF-α may also augment adherence of *P. gingivalis* as well as

298   that of leukocytes in part through inducing E-selectin expression. Weibel–Palade

299   bodies (WPBs) are endothelial granules that store von Willebrand factor (VWF) and other

300   vascular modulators (50) (48). Endothelial cells secrete WPBs in response to vascular

301   injury, releasing VWF, which triggers platelet rolling. Endothelial exocytosis is one of the

302   earliest responses to vascular damage and plays a pivotal role in thrombosis

303   and inflammation (29). In this study we demonstrated that *P. gingivlis* interaction with

304   endothelial cells via E-selectin activates the endothelial cells and enhances endothelial

305   exocytosis (Figure 4) and may enhance atherogenesis and thrombosis (e.g., Buerger disease)

306   (7) (23).

307   Pgm6/7 in *P. gingivalis*, which shares a low homology with *E. coli*

308   OmpA, exists as a heterotrimer comprising Pgm6 and Pgm7 and plays a role in the outer

309   membrane integrity in this organism. OmpA in *E. coli* K1 has been reported to interact with

310   a glycoprotein (Ecgp) of human brain microvascular endothelial cells for

311   invasion. Therefore, *P. gingivalis* invasion into endothelial cells should be investigated in

312   the near future, especially as to whether Pgm6/7 is involved in the invasion. How does

313   Pgm6/7 bind to E-selectin?   The adhesion activity of E-selectin is mediated primarily by the

314   binding of sialyl Lewis X on the leukocyte to the carbohydrate-binding domain.   E-selectin

315   recognizes the carbohydrate structure of sLeX.   Pgm6/7 is also a glycoprotein and therefore

316   it may bind to E-selectin through its carbohydrate side chain.   However, we need additional

317   experiments for revealing the mechanism.

318   Collectively, in the present study, we clarified a new host-pathogen interaction: an

319   interaction between Pgm6/7, a major outer membrane protein of *P. gingivalis,* and E-selectin

320   of activated endothelial cells.   This finding raises the possibility that chronic infection of the

321   vasculature by pathogens such as *P. gingivalis* could exacerbate systemic vascular diseases,

322   such as coronary heart disease, stroke, and diabetes mellitus.

323